TEN-VERTEX POLYHEDRAL RHODADICARBABORANE CHEMISTRY.* MOLECULAR STRUCTURE, NMR PROPERTIES, AND CLUSTER DYNAMIC BEHAVIOUR OF [2,2,2-$(PPh_3)_2$H-*closo*-2,1,6-$RhC_2B_7H_9$]

Karl NESTOR[a], Michael MURPHY[b], Bohumil ŠTÍBR[c], Trevor R. SPALDING[b], Xavier L. R. FONTAINE[a], Mark THORNTON-PETT[a] and John D. KENNEDY[a]

[a] *School of Chemistry, University of Leeds, Leeds LS2 9JT, England*

[b] *Department of Chemistry, University College Cork, Eire*

[c] *Institute of Inorganic Chemistry, Academy of Sciences of the Czech Republic, 250 68 Řež near Prague, The Czech Republic*

Received June 22, 1992
Accepted July 13, 1992

The compound previously described as [6,6,6-$(PPh_3)_2$H-*closo*-6,2,3-$RhC_2B_7H_9$] is shown by detailed multielement NMR studies and single-crystal X-ray diffraction analysis to be its isomer [2,2,2-$(PPh_3)_2$H-*closo*-2,1,6-$RhC_2B_7H_9$]. Crystals (from pentane–diethyl ether) were monoclinic, space group $P2_1/n$, with $Z = 4$, and with $a = 1\ 222.2(1)$ pm, $b = 1\ 598.7(2)$ pm, $c = 1\ 836.7(1)$ pm, and $\beta = 91.86(1)°$. The structure was refined to $R(R_w)$ 0.0295(0.0414) using 6 819 observed data [$I > 2.0\ \sigma(I)$] out of 8 541 collected at 200 K. The $\{RhC_2B_7\}$ cluster structure is to a first approximation classically *closo*, with the metal and two carbon atoms in adjacent 2, 1, and 6 positions, respectively. Both enantiomers exist in the unit cell, and variable temperature NMR studies show that the molecule is fluxional ($\Delta G^{\ddagger}_{355} \sim 60$ kJ mol^{-1}) between enantiomers via a diamond-square diamond cluster rearrangement.

Our three laboratories have individual and collaborative interests in the development of the systematics and thereby the understanding of polyhedral borane, carborane, and heteroborane cluster chemistry, and metallaborane, metallacarborane, and metallaheteroborane cluster chemistry. In respect of work on clusters containing metal atoms, some of our effort has been directed at attempting to facilitate intercomparisons by the use of selected "standard" later-transition-element centered units such as $\{Ru(\eta^6\text{-}C_6Me_6)\}$, $\{Rh(\eta^5\text{-}C_5Me_5)\}$, $\{Pt(PMe_2Ph)_2\}$, $\{RhH(PPh_3)_2\}$, $\{Ir(PPh_3)_2\}$, and $\{Ir(CO)(PPh_3)_2\}$. In this general context, while developing the systematics and perceptions within the areas of twelve-vertex $\{MC_2B_9\}$ (refs[1-4]) and eleven-vertex $\{MC_2B_8\}$ cluster chemistry[5-9], we have now started to examine ten-vertex $\{MC_2B_7\}$ chemistry[10,11]. Accordingly, we have been assessing known $\{MC_2B_7\}$ work[10-32] and during the course of this

* Contribution No. 27 from the Řež–Leeds Anglo-Czech Polyhedral Collaboration (A.C.P.C.).

assessment we found a puzzle within the published literature on *closo*-{RhC_2B_7} species, which this present paper now resolves. The numbering scheme for the ten-vertex *closo* cluster type is in structure *I*.

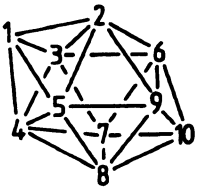

I

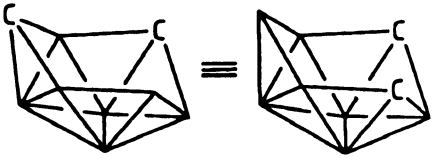

IIA *IIB*

The pioneering work in the area of *closo*-{MC_2B_7} cluster compounds was initiated a quarter of a century ago in the laboratory of Hawthorne and co-workers[12,14,16 – 19,22] with syntheses derived from [*arachno*-4,6-$C_2B_7H_{13}$] (schematic cluster configuration *II*) and its actual or incipient anions [4,6-$C_2B_7H_{12}$]$^-$ and [4,6-$C_2B_7H_{11}$]$^{2-}$. Examples of such syntheses which are relevant to this present paper are contained in some of the work using cobalt as the metal centre[12 – 14]. Thus the reaction of the [4,6-$C_2B_7H_{11}$]$^{2-}$ dianion with $CoCl_2$ in the presence of the [C_5H_5]$^-$ anion yielded [2-(η^5-C_5H_5)-*closo*-2,1,6-$CoC_2B_7H_9$] (schematic cluster configuration *III*) in 36% yield together with a 65% yield of the anionic species [$Co(C_2B_7H_{11})_2$]$^-$ which has the more symmetrical 2,6,9 cluster configuration *IV*. Mechanistically it can be seen that *III* and *IV* can be derived quite simply by metal capping and cluster closure on *IIA* and *IIB*, respectively.

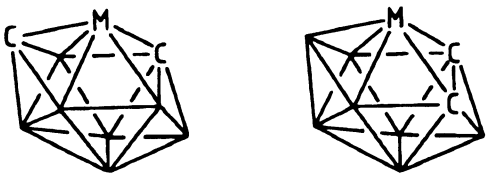

III *IV*

Subsequently the same laboratory reported[22,26] the reaction between [$RhCl(PPh_3)_3$] and the [4,6-$C_2B_7H_{12}$]$^-$ anion to yield a *closo* rhodadicarbaborane of formulation [$(PPh_3)_2HRhC_2B_7H_9$]. From the cobaltadicarbaborane work just cited there was a precedent for the formation of both the 2,1,6 and 2,6,9 configurations in this type of synthesis. The rhodadicarbaborane had a 1 : 2 : 2 : 1 : 1 : 1 relative intensity pattern in the ^{11}B NMR spectrum, and it was therefore proposed[26] that the cluster had the symmetrical {2,6,9-RhC_2B_7} configuration *IV* even though it was recognized that this would require a boron atom in the lower-connectivity 1-position adjacent to the metal atom which would generally be expected to result in a low-field ^{11}B chemical shift[16],

contrary to the observations for this particular compound (see also Table I below). A consideration of general ^{11}B NMR shielding patterns[10-14,16-18,22,25,26,29-32] within known {*closo*-MC_2B_7} cluster types, however, suggested to us that the {2,6,9-RhC_2B_7} configuration was perhaps not the correct one, and therefore we undertook a reexamination of the rhodacarbaborane in order unequivocally to establish the structure and hence the reason for the symmetry in the ^{11}B NMR spectrum.

RESULTS AND DISCUSSION

The synthesis of the rhodadicarbaborane was readily effected from [$RhCl(PPh_3)_3$] and [*arachno*-4,6-$C_2B_7H_{13}$] (Eq. (*A*)), using essentially the same principles as Jung and Hawthorne[22,26]. Different bases (see Experimental) were utilized in the two of our laboratories which undertook the syntheses. With triethylamine as base, the rhodadicarbaborane was isolated in 40% yield, but with N,N,N',N'-tetramethylnaphthalene-1,8-diamine (TMND) a somewhat higher yield of 64% was obtained. The product, a yellow crystalline solid[26], was readily purified by chromatography.

$$[RhCl(PPh_3)_3] + [C_2B_7H_{13}] + \text{base} \longrightarrow$$

$$[(PPh_3)_2HRhC_2B_7H_9] + H_2 + \text{base}\,H^+Cl^- + PPh_3 \qquad (A)$$

The measured NMR spectra are in Table I. The ^{11}B chemical shift data are essentially identical to those reported previously[26] and the previously reported 1 : 2 : 2 : 1 : 1 ^{11}B relative intensity pattern was clearly apparent. However, in the resolution-enhanced proton-coupled 128 MHz ^{11}B spectrum there was some asymmetry in the two peaks of relative intensity two, which suggested that each may consist of two near-coincident but different resonances. Selective ^1H-{^{11}B} spectroscopy thence revealed that this was indeed the case, showing that there are two distinct ^1H resonances associated with each of these two ^{11}B NMR peaks, and thereby confirming that there are two distinct BH groups in each case. The compound therefore has an asymmetric structure, at variance with the original[26] conclusion.

Reference to more recent literature[10] in fact shows that the ^{11}B and ^1H shielding patterns (Table I and and Fig. 1) are strikingly similar to those unequivocally established for the {2,1,6-MC_2B_7} species [2-(η^6-C_6Me_6)-*closo*-2,1,6-$RuC_2B_7H_9$] (data also included in Table I and Fig. 1 for comparison). In particular the very close similarities of the ^{11}B shieldings (centre two traces in the lower diagram of Fig. 1) permit the assignments in Table I which are generally also confirmed by the pairwise coalescences (bottom and top traces in the lower diagram of Fig. 1) arising from the cluster fluxionality as described below (see Scheme 1 and Fig. 3). The ^1H NMR data are also notably similar, with close groupings, for equivalent BH positions in the two species, in a $\delta(^1H) : \delta(^{11}B)$ correlation plot (upper diagram in Fig. 1) (it is of interest to note

parenthetically that the relatively steep $\delta(^1H) : \delta(^{11}B)$ correlation slope of ca 1 : 10 for these two *closo* species supports the suggestion[6,33,34] that steeper correlations may often be diagnostic of *closo* behaviour in clusters of intermediate size, as distinct from *nido* and *arachno* behaviours which are more often associated[34 - 36] with shallower $\delta(^1H) : \delta(^{11}B)$ correlation slopes in the region approximately 1 : 14 to 1 : 20). In sum these comparative NMR data strongly suggest the [2,2,2-$(PPh_3)_2$H-*closo*-2,1,6-$RhC_2B_7H_9$] configuration *III* for the rhodadicarbaborane.

This conclusion was confirmed by the results of a single crystal X-ray diffraction analysis, for which crystals were obtained by diffusion of pentane into a solution in diethyl ether. A drawing of the crystallographicaly determined molecular structure is in Fig. 2, with selected interatomic distances and angles in Tables II and III, respectively. Important atomic coordinates are listed in Table IV associated with the Experimental.

The compound is clearly seen to have chiral [2,2,2-$(PPh_3)_2$H-*closo*-2,1,6-$RhC_2B_7H_9$] configuration. There was no significant crystallographic disorder of the type that would result from the interchange of C(6) and B(9), and the crystal structure was such that

TABLE I

NMR data for [2-(η^6-C_6Me_6)-*closo*-2,1,6-$RuC_2B_7H_9$] (data from ref.[10])and [2,2,2-$(PPh_3)_2$H-*closo*-2,1,6-$RhC_2B_7H_9$] (this work) in CD_2Cl_2 solution at 294 – 297 K

Assigment	[$(C_6Me_6)RuC_2B_7H_9$]		[$(PPh_3)_2HRhC_2B_7H_9$][a]	
	$\delta(^{11}B)$	$\delta(^1H)$	$\delta(^{11}B)$	$\delta(^1H)$
10	16.5[b]	4.87	23.8[c]	4.51
4	-6.5[d]	1.81	-6.3[e]	2.38
9	-6.5	2.48	-6.3	1.82
5	-24.1[b]	-0.22	-19.7[c]	1.07
8	-21.5	0.32	-19.7	0.94
3	-24.1	0.58	-22.5	0.56
7	-33.7[d]	-0.03	-33.9[e]	0.18
1	–	5.60	–	4.62
6	–	2.39	–	1.15
2	–	[2.04][f]	–	-11.97[g]

[a] $\delta(^{31}P)$ +43.3 [$^1J(^{103}Rh\text{-}^{31}P)$ 112.5 Hz] and +41.0 [$^1J(^{103}Rh\text{-}^{31}P)$ 131 Hz]; no coupling $^2J(^{31}P\text{-}^{31}P)$ apparent at $w_{1/2}$ ca 30 Hz. [b] These peaks coalesce at $\delta(^{11}B)$ -3.2 at high temperatures ($CD_3C_6D_5$ solution). [c] These peaks coalesce at $\delta(^{11}B)$ ca +3 at high temperatures; coalesce temperature ca 358 K at 9.35 T ($CD_3C_6D_5$ solution). [d] These peaks coalesce at $\delta(^{11}B)$ -19.6 at high temperatures ($CD_3C_6D_5$ solution). [e] These peaks coalesce at $\delta(^{11}B)$ ca -19 at high temperatures; coalesce temperature ca 353 K at 9.35 T ($CD_3C_6D_5$ solution). [f] Refers to C_6Me_6 protons. [g] Doublet [$^1J(^{103}Rh\text{-}^1H)$ 16 Hz] of triplets [$^3J(^{31}P\text{-}^1H)$ (mean) ca 25 Hz].

both enantiomers were present in the unit cell. The exopolyhedral $\{RhH(PPh_3)_2\}$ coordination sphere was similarly oriented to that previously found for the $\{RhH(PEt_3)_2\}$ analogue[30], with the rhodium hydride approximately trans to the carbon atom C(6) in the tropical belt. In this regard there is an interesting contrast within the $\{CoH(PEt_3)_2\}$ analogue which adopts a coordination sphere configuration that has the hydride trans to the apical (axial) carbon atom C(1). In general terms the compound is classically *closo*, and thereby has the bicapped square antiprismatic $[B_{10}H_{10}]^{2-}$ structural motif[37]. The "octahedral" rhodium(III) centre $\{RhH(PPh_3)_2\}$ formally contributes three orbitals and two electrons to the Wadian cluster bonding scheme[38]. However, as we have recently noted for other ostensibly classically *closo* ten-vertex heteroboranes[39,40], there is some opening towards *isonido*, manifested in this case by a somewhat long C(6)–B(9) linkage of 180.3(5) pm. This opening phenomenon is adequately discussed elsewhere[39]. Two other notable features within the *closo* structure are the short Rh(2)–C(1) distance at 208.9(4) pm and the long Rh(2)–C(6) distance of

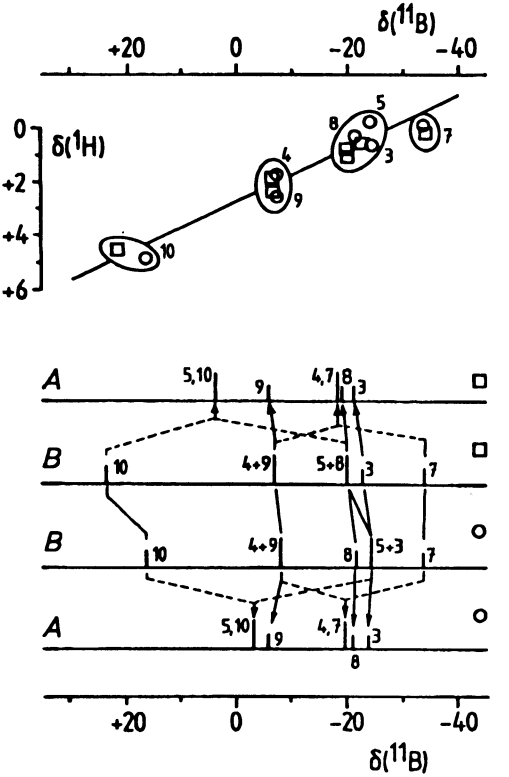

FIG. 1

NMR data for $[2,2,2\text{-}(PPh_3)_2H\text{-}closo\text{-}2,1,6\text{-}RhC_2B_7H_9]$ (○) and, for comparison purposes, $[2\text{-}(\eta^6\text{-}C_6Me_6)\text{-}closo\text{-}2,1,6\text{-}RuC_2B_7H_9]$ (□) (data from ref.[10]). The lower diagram represents the chemical shifts (in ppm) and relative intensities in the ^{11}B spectra at (*A*) high and (*B*) low temperatures, with lines joining equivalent positions. The upper diagram (same scale in $\delta(^{11}B)$) is a plot of $\delta(^1H)$ versus $\delta(^{11}B)$ for the BH units in the two compounds; the assignments are those for the ruthenium compound (□) and the line drawn has slope $\delta(^1H) : \delta(^{11}B)$ 1 : 10, intercept +2.75 ppm in $\delta(^1H)$

236.7(4) pm. The latter is longer than the rhodium–boron distances to B(5) and B(9) of 232.8(5) and 220.5(4) pm, respectively, and very similar to the Rh(2)–B(3) distance of 236.7(4) pm. It may indicate incipient opening to true *nido* as discussed in the next paragraph. The two rhodium– phosphorus distances are mutually similar at 232.7(3) and 231.4(3) pm, and are typical of rhodium–triphenylphosphine linkages. The ranges of interboron and boron–carbon distances are 168.6(6) to 184.9(6) and 159.1(6) to 180.3(5) pm, respectively.

An interesting feature of [2,2,2-$(PPh_3)_2$H-*closo*-2,1,6-$RhC_2B_7H_9$] also revealed by NMR spectroscopy is that the {RhC_2B_7} cluster is fluxional between enantiomers. This is manifested by a now genuine 2 : 1 : 2 : 1 : 1 relative intensity pattern in the 128 MHz ^{11}B NMR spectrum at higher temperatures (> 360 K), indicating fluxionality but with exchange only involving two particular site pairs. Intermediate temperatures (ca 350 – 360 K) showed that the exchange occured within each of the pairs B(5)/B(10) and B(4)/B(7) (Fig. 1 and Table I), and again the extreme similarity of the behaviour to that of [2-(η^6-C_6Me_6)-*closo*-2,1,6-$RuC_2B_7H_9$] also in Fig. 1 and Table I) confirmed that the fluxionality was exactly analogous to that previously established[10] for the latter compound. One possible mechanism could proceed via two concerted or sequential diamond–square-diamond rearrangements involving the Rh(2)C(1)B(5)B(9) and Rh(2)C(6)B(10)B(9) units (Fig. 3). If so the process could well involve square-faced intermediates of "*isonido*" structure (Scheme 1)[39,40] with some additional opening towards true *nido* (hatched lines in Scheme 1) at the reaction mid-coordinate. The longer C(6)–B(9) and Rh(2)–C(6) linkages alluded to in previous paragraph respectively indicate some distortion towards these *isonido* and *nido* intermediate structures even in the ground state. NMR spectroscopy as the intermediate temperatures determi-

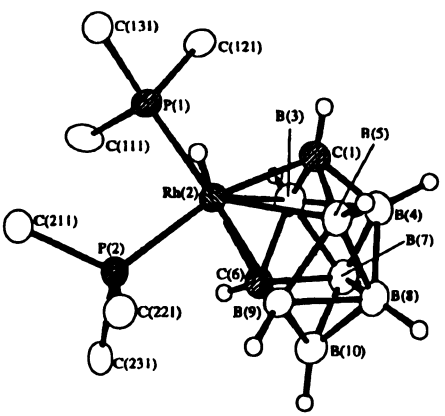

FIG. 2
Drawing of the crystallographically determined molecular structure of [2,2,2-$(PPh_3)_2$H-*closo*-2,1,6-$RhC_2B_7H_9$] with the P-phenyl atoms, apart from the *ipso* carbon ones, omitted for clarity[47]. Because the compound crystallizes in a centrosymmetric space group the other enantiomer is also present in the unit cell. The fluxionality between enantiomers (Scheme 1 and Fig. 3) involves reversible migration of C(1) to the 9-, B(3) to the 5-, B(4) to the 7-, B(5) to the 10-, C(6) to the 1-, B(7) to the 4-, B(8) to the 7-, B(9) to the 6-, and B(10) to the 3-position, whereas Rh(2) remains at the 2-position. Thus B(3), B(8) and B(9) are each exchanged to a chemically equivalent although enantiomeric position, whereas the B(5)B(10), B(4)B(7) and C(1)C(6) pairs each exchange between two chemically different sites

ned coalescence temperatures for the exchange process (Table I), giving calculated values for $\Delta G^{\neq}$ of 60.2 ± 1.0 and 60.6 ± 1.0 kJ mol^{-1} at 353 and 358 K, respectively. The mean value of ca 60.4 kJ mol^{-1} at 355 K is somewhat greater than the value $\Delta G^{\neq}_{272}$ of ca 45 kJ mol^{-1} for the {Ru(η^6-C_6Me_6)} compound[10], but only marginally greater than that reported[10] for the {Rh(η^5-C_5Me_5)} congener [2-(η^5-C_5Me_5)-*closo*-2,1,6-$RhC_2B_7H_9$] with $\Delta G^{\neq}_{345}$ ca 58 kJ mol^{-1}. These values are perhaps not too different and it is thereby interesting that the electronic effects on the cluster of the three different metal centres {Ru(η^6-C_6Me_6)}, {Rh(η^5-C_5Me_5)}, and {RhH(PPh_3)$_2$} are markedly similar in this cluster type, a factor also reinforced by the extreme similarities of the ^{11}B and ^{1}H chemical shifts themselves (e.g. Fig. 1) in the non-exchanging low-temperature spectra.

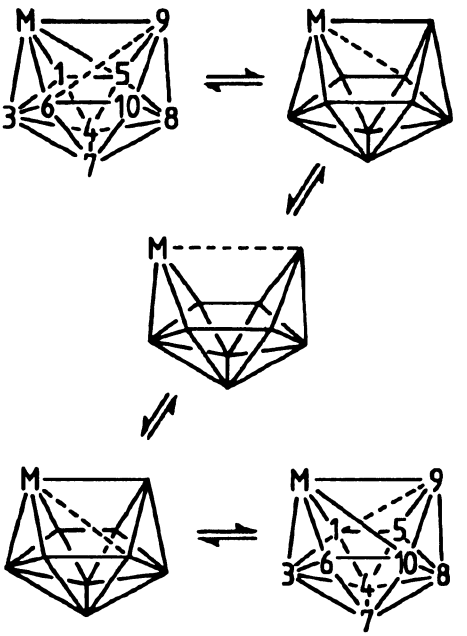

SCHEME 1

In the context of this fluxionality it is appropriate to note here that an alternative dynamic process in [2,2,2-(PPh_3)$_2$H-*closo*-2,1,6-$RhC_2B_7H_9$] was reported in the original work[26] to involve fast triphenylphosphine exchange. This exchange was reported to be manifested in (i) broad P-phenyl proton resonances and (ii) a lack of an observable hydride resonance in the ^{1}H spectrum in the absence of excess PPh_3. We did not see any evidence for this type of behaviour in our particular experiments, however. Thus, pure samples of [2,2,2-(PPh_3)$_2$H-*closo*-2,1,6-$RhC_2B_7H_9$] showed (i) two ^{31}P resonances, each with different couplings $^1J(^{103}Rh$-$^{31}P)$ as expected for a non-dissociating asymmetric structure; in addition, (ii) the P-phenyl ^{1}H resonances were sharp, and,

furthermore, (iii) we also observed the Rh–H proton multiplet at $\delta(^1H)$ ca −12 ppm to be reasonably sharp ($w_{1/2}$ ca 5 Hz), this 5 Hz broadening presumably arising from transoid ^2J and ^3J couplings to ^{11}B of up to a few Hz. In accord with this last presumption, this last resonance was in fact sharpened in the ^1H-{^{11}B} experiments. Interstingly, this sharpening was most marked when the $^{11}B(5)(10)$ and, to a lesser extent, when the $^{11}B(4)(7)$ positions were irradiated, implying larger $^3J(^{11}B\text{-}B\text{-}Rh\text{-}^1H)$ values than $^2J(^{11}B\text{-}Rh\text{-}^1H)$.

EXPERIMENTAL

Preparation of [2,2,2-$(PPh_3)_2$H-*closo*-2,1,6-$RhC_2B_7H_9$]

The route chosen was essentially similar to that of Jung and Hawthorne[22,26], with two variations in detail being utilized, as follows (*arachno*-4,6-$C_2B_7H_{13}$ being prepared essentially according to ref.[41]).

a) *With NEt_3 as base.* Equimolar amounts of 4,6-$C_2B_7H_{13}$ (34 mg, 303 μmol) and [$RhCl(PPh_3)_3$] (280 mg, 303 μmol) were added to CH_2Cl_2 (25 ml) in a nitrogen atmosphere. Triethylamine (42 μl, 303 μmol) was added and the reaction mixture became brown. It was then stirred for 3 h, the solution reduced in volume (rotary film evaporator, water-pump pressure, 25 °C) and the resulting liquid subjected to preparative TLC on silica (GF254, Merck) using CH_2Cl_2–heptane (3 : 2) as eluting liquid. One major (yellow) component was obtained, recrystallized from CH_2Cl_2, and identified as [2,2,2-$(PPh_3)_2$H-*closo*-2,1,6-$RhC_2B_7H_9$] (90 mg, 120 μmol, 40%) by IR spectroscopy [ν_{max} 2 521 s, 2 503 msh (B–H) and 2 080 w (Rh–H)] and multielement NMR spectroscopy (Table I) as described in the text.

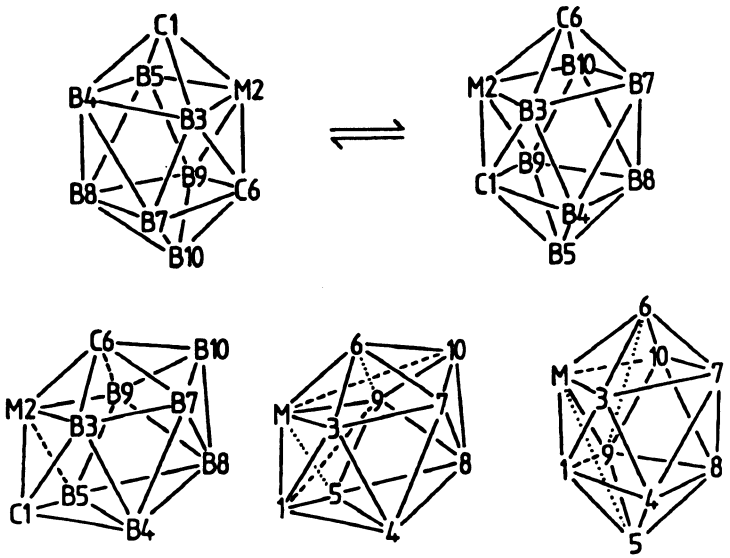

FIG. 3

Diagram showing how the proposed fluxionality (see also Scheme 1) interchanges enantiomers and gives the positional changes summarized in the caption to Fig. 2, together with the NMR coalescences summarized in Fig. 1 (lower diagrams)

b) With TMND as base. Equimolar amounts of 4,6-$C_2B_7H_{13}$ (28 mg, 250 μmol), [$RhCl(PPh_3)_3$] (230 mg, 250 μmol), and TMND (53 mg, 250 μmol) were stirred in solution in CH_2Cl_2 (10 ml) in a nitrogen atmosphere for 12 h, during which time a slight darkening of the initial orange colour occured. The solution was then reduced in volume to ca 5 ml (rotary evaporator, water-pump pressure, 25 °C) and the resulting liquid subjected to preparative TLC on silica (GF254, Merck) using CH_2Cl_2–hexane (3 : 2) as eluting liquid. One yellow mobile component (R_F 0.65) was obtained, which was extracted from the silica by washing with CH_2Cl_2 (ca 20 ml). Addition of an equal volume of hexane, followed by slow evaporation (rotary evaporator, water-pump pressure, 25 °C) yielded a bright yellow precipitate (119 mg, 160 μmol, 65%) identified as [2,2,2-$(PPh_3)_2$H-*closo*-2,1,6-$RhC_2B_7H_9$] as above. Crystals suitable for single-crystal X-ray diffraction work were grown by slow diffusion of pentane into a solution in diethyl ether.

In both routes no attempt was made to optimize yields, the principal purpose being to obtain pure samples for NMR spectroscopy and single-crystal X-ray diffraction analysis. The compound was reasonably stable in CD_2Cl_2 solution at ambient temperatures for extended periods, but $CD_3C_6D_5$ solutions used for the high-temperature investigations of fluxionality rapidly changed from yellow to dark red at 350 K, and the ^{11}B NMR spectra showed extensive signs of non-specific decomposition after ca 20 min at this temperature.

TABLE II

Selected interatomic distances (in pm) for [2,2,2-$(PPh_3)_2$H-*closo*-2,1,6-$RhC_2B_7H_9$], with estimated standard deviations (e.s.d.'s) in parentheses

Atoms	Distance	Atoms	Distance
P(1)–Rh(2)	232.7(3)	P(2)–Rh(2)	231.4(3)
C(1)–Rh(2)	208.9(4)	B(3)–Rh(2)	236.7(5)
B(5)–Rh(2)	232.8(5)	C(6)–Rh(2)	236.7(4)
B(9)–Rh(2)	220.5(4)	H(2)–Rh(2)	150.2(29)
C(111)–P(1)	183.9(3)	C(121)–P(1)	184.2(3)
C(131)–P(1)	183.4(3)		
C(211)–P(2)	183.5(3)	C(221)–P(2)	183.7(3)
C(231)–P(2)	184.0(3)		
B(3)–C(1)	161.4(6)	B(4)–C(1)	161.8(6)
B(5)–C(1)	159.1(6)	H(1)–C(1)	90.9(28)
C(6)–B(3)	169.8(6)	B(7)–B(3)	182.1(6)
H(3)–B(3)	108.1(31)	B(3)–B(4)	184.9(6)
B(7)–B(4)	174.9(6)	B(8)–B(4)	178.7(6)
H(4)–B(4)	113.7(29)	B(4)–B(5)	184.5(6)
B(8)–B(5)	183.9(6)	B(9)–B(5)	183.9(6)
H(5)–B(5)	111.1(25)	B(7)–C(6)	173.7(5)
B(9)–C(6)	180.3(5)	B(10)–C(6)	159.7(5)
H(6)–C(6)	91.2(28)	H(7)–B(7)	111.9(28)
B(10)–B(7)	168.7(6)	B(7)–B(8)	182.0(6)
B(10)–B(8)	168.6(6)	H(8)–B(8)	105.6(33)
B(8)–B(9)	183.7(6)	B(10)–B(9)	172.3(6)
H(9)–B(9)	103.7(27)	H(10)–B(10)	106.5(25)

TABLE III

Selected angles (in °) between interatomic vectors for [2,2,2-$(PPh_3)_2$H-*closo*-2,1,6-$RhC_2B_7H_9$], with e.s.d.'s in parentheses

Atoms	Angle	Atoms	Angle
P(2)–Rh(2)–P(1)	99.3(1)	C(1)–Rh(2)–P(1)	97.5(2)
C(1)–Rh(2)–P(2)	162.9(1)	B(3)–Rh(2)–P(1)	92.6(2)
B(3)–Rh(2)–P(2)	139.5(1)	B(3)–Rh(2)–C(1)	41.9(1)
B(3)–Rh(2)–B(5)	66.8(2)	B(5)–Rh(2)–P(1)	136.9(1)
B(5)–Rh(2)–P(2)	121.2(2)	B(5)–Rh(2)–C(1)	41.8(1)
C(6)–Rh(2)–P(1)	116.6(2)	C(6)–Rh(2)–P(2)	99.1(2)
C(6)–Rh(2)–C(1)	75.8(2)	C(6)–Rh(2)–B(3)	42.0(1)
C(6)–Rh(2)–B(5)	73.6(2)	B(9)–Rh(2)–P(1)	162.9(1)
B(9)–Rh(2)–P(2)	84.5(2)	B(9)–Rh(2)–C(1)	80.2(2)
B(9)–Rh(2)–B(3)	74.3(2)	B(9)–Rh(2)–B(5)	47.8(1)
B(9)–Rh(2)–C(6)	46.3(1)	H(2)–Rh(2)–P(1)	82.5(11)
H(2)–Rh(2)–P(2)	79.7(11)	H(2)–Rh(2)–C(1)	99.7(11)
H(2)–Rh(2)–B(3)	140.5(10)	H(2)–Rh(2)–B(5)	90.4(11)
H(2)–Rh(2)–C(6)	160.6(10)	H(2)–Rh(2)–B(9)	114.6(11)
B(3)–C(1)–Rh(2)	78.3(2)	B(3)–C(1)–B(4)	69.8(3)
B(3)–C(1)–B(5)	107.5(3)	B(4)–C(1)–Rh(2)	123.6(3)
B(4)–C(1)–B(5)	70.2(3)	B(5)–C(1)–Rh(2)	77.2(2)
B(3)–C(6)–Rh(2)	69.0(2)	B(7)–C(6)–Rh(2)	119.6(3)
B(7)–C(6)–B(3)	64.0(3)	B(7)–C(6)–B(9)	95.0(3)
B(9)–C(6)–Rh(2)	62.1(2)	B(9)–C(6)–B(3)	104.1(3)
B(10)–C(6)–Rh(2)	122.3(3)	B(10)–C(6)–B(3)	119.8(3)
B(10)–C(6)–B(7)	60.6(3)	B(10)–C(6)–B(9)	60.5(2)
B(5)–B(9)–Rh(2)	69.6(2)	C(6)–B(9)–Rh(2)	71.6(2)
C(6)–B(9)–B(5)	101.0(3)	B(8)–B(9)–Rh(2)	118.8(3)
B(8)–B(9)–B(5)	60.0(2)	B(8)–B(9)–C(9)	85.7(3)
B(10)–B(9)–Rh(2)	125.0(3)	B(10)–B(9)–B(5)	111.8(3)
B(10)–B(9)–C(6)	53.8(2)	B(10)–B(9)–B(8)	56.4(3)
B(9)–B(10)–C(6)	65.7(3)	B(8)–B(10)–C(6)	97.9(3)
B(8)–B(10)–B(9)	65.2(3)	B(7)–B(10)–C(6)	63.8(3)
B(7)–B(10)–B(8)	65.3(3)	B(7)–B(10)–B(9)	99.9(3)
H(10)–B(10)–C(6)	126.7(14)	H(10)–B(10)–B(7)	132.6(13)
H(10)–B(10)–B(8)	135.4(13)	H(10)–B(10)–B(9)	127.2(14)

TABLE IV

Non-hydrogen and cluster-hydrogen fractional atomic coordinates (. 10^4) for [2,2,2-$(PPh_3)_2$H-*closo*-2,1,6-$RhC_2B_7H_9$], with e.s.d.'s in parentheses

Atom	*x*	*y*	*z*	U_{iso}/U_{eq} [a]
Rh(2)	4419.1(1)	2102.1(1)	1018.0(1)	23.8(1)
P(1)	6131.5(5)	2125.4(4)	500.7(3)	28.0(2)
P(2)	4936.0(4)	2406.3(4)	2211.7(3)	25.8(1)
C(1)	3509(2)	1755(2)	84(1)	36(1)
B(3)	3568(2)	2758(2)	-8(1)	36(1)
B(4)	2308(2)	2125(2)	-126(2)	37(1)
B(5)	2693(2)	1562(2)	721(2)	33(1)
C(6)	3266(2)	3265(2)	773(1)	30(1)
B(7)	2203(2)	3177(2)	127(2)	37(1)
B(8)	1616(2)	2366(2)	691(2)	35(1)
B(9)	2766(2)	2451(2)	1356(1)	29(1)
B(10)	2030(2)	3298(2)	1028(2)	36(1)
C(111)	6864(1)	3116(1)	662(1)	38(1)
C(112)	7874(1)	3154(1)	1036(1)	50(1)
C(113)	8367(1)	3927(1)	1178(1)	71(1)
C(114)	7850(1)	4662(1)	944(1)	71(1)
C(115)	6840(1)	4624(1)	569(1)	62(1)
C(116)	6347(1)	3851(1)	428(1)	50(1)
C(121)	6089(1)	1993(1)	-496(1)	34(1)
C(122)	6388(1)	2618(1)	-982(1)	40(1)
C(123)	6377(1)	2455(1)	-1728(1)	52(1)
C(124)	6067(1)	1667(1)	-1989(1)	57(1)
C(125)	5769(1)	1043(1)	-1504(1)	52(1)
C(126)	5779(1)	1206(1)	-757(1)	43(1)
C(131)	7133(1)	1290(1)	679(1)	33(1)
C(132)	8191(1)	1371(1)	425(1)	45(1)
C(133)	8936(1)	714(1)	512(1)	59(1)
C(134)	8622(1)	-23(1)	855(1)	60(1)
C(135)	7564(1)	-104(1)	1109(1)	57(1)
C(136)	6820(1)	553(1)	1021(1)	46(1)
C(211)	6385(1)	2302(1)	2489(1)	31(1)
C(212)	7069(1)	2976(1)	2663(1)	43(1)
C(213)	8163(1)	2837(1)	2867(1)	54(1)
C(214)	8574(1)	2023(1)	2896(1)	55(1)
C(215)	7890(1)	1348(1)	2721(1)	59(1)
C(216)	6796(1)	1488(1)	2517(1)	49(1)
C(221)	4377(1)	1716(1)	2907(1)	29(1)
C(222)	4739(1)	1812(1)	3630(1)	37(1)

TABLE IV
(*Continued*)

Atom	*x*	*y*	*z*	U_{iso}/U_{eq} [a]
C(223)	4375(1)	1266(1)	4163(1)	42(1)
C(224)	3648(1)	624(1)	3973(1)	44(1)
C(225)	3286(1)	527(1)	3250(1)	41(1)
C(226)	3650(1)	1074(1)	2717(1)	33(1)
C(231)	4570(1)	3470(1)	2499(1)	30(1)
C(232)	4955(1)	4133(1)	2084(1)	38(1)
C(233)	4707(1)	4955(1)	2273(1)	44(1)
C(234)	4074(1)	5114(1)	2876(1)	47(1)
C(235)	3690(1)	4452(1)	3290(1)	44(1)
C(236)	3938(1)	3630(1)	3102(1)	36(1)
H(1)	3780(21)	1372(17)	-229(14)	40(7)
H(2)	4799(22)	1255(17)	1274(14)	48(8)
H(3)	4049(25)	3084(18)	-402(16)	54(9)
H(4)	1850(24)	1869(18)	-626(16)	54(9)
H(5)	2444(20)	916(15)	862(13)	35(6)
H(6)	3678(21)	3734(17)	848(14)	39(7)
H(7)	1896(22)	3655(17)	-275(15)	48(8)
H(8)	821(26)	2165(17)	816(17)	59(9)
H(9)	2720(20)	2489(16)	1918(14)	37(7)
H(10)	1665(19)	3781(15)	1338(13)	31(6)

[a] U_{eq} is defined as one third of the trace of the orthogonalized $\boldsymbol{U}_{ij}$ tensor.

NMR Spectroscopy

NMR spectroscopy was carried out on a Bruker AM400 instrument operating at ca 9.35 T, with the basic techniques as described in other recent papers from our laboratories[2,42,43]. Chemical shifts δ are given in ppm to high frequency (low field) of Ξ = 100 MHz ($SiMe_4$) for ^1H (quoted ±0.05 ppm), Ξ = 40.480730 MHz (nominally 85% H_3PO_4) for ^{31}P, and Ξ = 32.083971 MHz (nominally F_3BOEt_2 in $CDCl_3$) for ^{11}B (quoted ±0.5 ppm), Ξ being defined as in ref.[44].

X-Ray Crystallography

Single crystal X-ray diffraction. All crystallographic measurements were carried out on a Stoe STADI4 diffractometer operating in the ω/θ scan mode, using an on-line profile-fitting method[45] and graphite-monochromated Mo-K_α X-radiation (λ = 71.069 pm). The data set was corrected for absorption semiempirically using azimuthal psi scans. The structure was determined via standard heavy-atom (for the rhodium atom) and Fourier-difference techniques and was refined by full-matrix least-squares using the SHELX program system[46]. All non-hydrogen atoms were refined with anisotropic thermal parameters. The phenyl groups were treated as rigid bodies with idealized hexagonal symmetry (C–C = 139.5 pm). The phenyl

hydrogen atoms were included in calculated positions (C–H = 96 pm) and were refined with an overall isotropic thermal parameter. The cluster hydrogen-atom positions were located on a Fourier-difference map and were freely refined with isotropic thermal parameters. The weighting scheme $w = [\sigma^2(F_o) + 0.0002(F_o)^2]^{-1}$ was used. Final atomic coordinates are given in Table IV.

Crystal data. $C_{38}H_{40}B_7P_2Rh$, M = 737.3, monoclinic, space group $P2_1/n$, a = 1 222.2(1), b = 1 598.7(2), c = 1 836.7(1) pm, β = 91.86(1)°, U = 3.5870(6) nm^3, Z = 4, D_x = 1.37 Mg m^{-3}, μ = 5.22 cm^{-1}, $F(000)$ = 1 512.

Data collection. 4.0 < 2θ < 50.0°, 8 541 data collected, 6 819 with I > 2.0 σ(*I*) considered observed, T = 200 K.

Structure refinement. Number of parameters 402, R = 0.0295, R_w = 0.0414.

We thank the SERC (United Kingdom), the Royal Society (London), the Department of Education (Republic of Ireland), Academy of Sciences of the Czech Republic (Grant No. 43204), and Borax Research for support, and Johnson Matthey plc for the generous loan of some of the rhodium salts used in this work. We are also pleased to thank Dr T. S. Griffin and Dr D. M. Wagnerová for helpful interest.

REFERENCES

1. Bown M., Fontaine X. L. R., Greenwood N. N., Kennedy J. D., Plešek J., Štíbr B., Thornton-Pett M.: Acta Crystallogr., C *46*, 1010 (1990).
2. Fontaine X. L. R., Kennedy J. D., McGrath M., Spalding T. R.: Magn. Reson. Chem. *29*, 711 (1991).
3. Nestor K., Jelínek T., Fontaine X. L. R., Greenwood N. N., Kennedy J. D., Thornton-Pett M., Heřmánek S., Štíbr B.: J. Chem. Soc., Dalton Trans. *1990*, 681.
4. Ferguson G., Coughlan S., Spalding T. R., Fontaine X. L. R., Kennedy J. D., Štíbr B.: Acta Crystallogr., C *46*, 1402 (1990).
5. Kennedy J. D., Thornton-Pett M., Štíbr B., Jelínek T.: Inorg. Chem. *30*, 4481 (1991).
6. Kennedy J. D., Štíbr B., Jelínek T., Fontaine X. L. R., Thornton-Pett M.: Collect. Czech. Chem. Commun., in press. (205/92)
7. Nestor K., Fontaine X. L. R., Greenwood N. N., Kennedy J. D., Thornton-Pett M., Plešek J., Štíbr B.: Inorg. Chem. *28*, 2219 (1989).
8. Nestor K., Kennedy J. D., Štíbr B., Thornton-Pett M., Zammitt G. S. A.: J. Organomet. Chem., in press.
9. Bown M., Fontaine X. L. R., Greenwood N. N., Kennedy J. D., Thornton-Pett M.: Organometallics *6*, 2254 (1987).
10. Bown M., Jelínek T., Štíbr B., Heřmánek S., Fontaine, X. L. R., Greenwood N. N., Kennedy J. D., Thornton-Pett M.: J. Chem. Soc., Chem. Commun. *1988*, 974.
11. Štíbr B., Baše K., Jelínek T., Fontaine X. L. R., Kennedy J. D., Thornton-Pett M.: Collect. Czech. Chem. Commun. *56*, 646 (1991).
12. Hawthorne M. F., George T. A.: J. Am. Chem. Soc. *89*, 7114 (1967).
13. George T. A., Hawthorne M. F.: J. Am. Chem. Soc. *90*, 1661 (1968).
14. Hawthorne M. F., George T. A.: J. Am. Chem. Soc. *91*, 5475 (1969).
15. St. Clair D., Zalkin A., Templeton D. H.: Inorg. Chem. *11*, 377 (1972).
16. Jones C. J., Francis J. N., Hawthorne M. F.: J. Am. Chem. Soc. *94*, 8391 (1972).
17. Evans W. J., Dunks G. B., Hawthorne M. F.: J. Am. Chem. Soc. *95*, 4565 (1973).
18. Dustin D. F., Evans W. J., Jones C. J., Wiersema R. J., Gong H., Chan S., Hawthorne M. F.: J. Am. Chem. Soc. *96*, 3085 (1974).
19. Callahan K. P., Lo F. Y., Strouse C. E., Sims A. L., Hawthorne M. F.: Inorg. Chem. *13*, 2842 (1974).

20. Green M., Spencer J. L., Stone F. G. A., Welch A. J.: J. Chem. Soc., Chem. Commun. *1974*, 571.
21. Green M., Howard J. A. K., Spencer J. L., Stone F. G. A.: J. Chem. Soc., Chem. Commun. 1974, 153.; J. Chem. Soc., Dalton Trans. *1975*, 2274.
22. Jung C. W., Hawthorne M. F.: J. Chem. Soc., Chem. Commun. *1976*, 499.
23. Friesen G. D., Barriola A., Todd L. J.: Chem. Ind. (London) *19*, 631 (1978).
24. Štíbr B., Heřmánek S., Plešek J., Baše K., Zakharova I. A.: Chem. Ind. (London) *11*, 468 (1980).
25. Jung C. W., Baker R. T., Knobler C. B., Hawthorne M. F.: J. Am. Chem. Soc. *102*, 5782 (1980).
26. Jung C. W., Baker R. T., Hawthorne M. F.: J. Am. Chem. Soc. *103*, 810 (1981).
27. Baker R. T., Hawthorne M. F.: Unpublished results; as quoted in ref.[32] of ref.[26].
28. Welch A. J.: J. Am. Chem. Soc., Dalton Trans. *1975*, 2270.
29. Barker G. K., Garcia M. P., Green M., Pain G. N., Stone F. G. A., Jones S. K. R., Welch A. J.: J. Chem. Soc., Chem. Commun. *1981*, 652.
30. Barker G. K., Garcia M. P., Green M., Pain G. N., Stone F. G. A., Basset J.-M., Welch A. J.: J. Chem. Soc., Chem. Commun. *1981*, 653.
31. Hanusa T. P., Huffman J. C., Curtis T. L., Todd L. J.: Inorg. Chem. *24*, 787 (1985).
32. Briguglio J. J., Sneddon L. G.: Organometallics *5*, 327 (1986).
33. Ferguson G., Kennedy J. D., Fontaine X. L. R., Faridoon, Spalding T. R.: J. Chem. Soc., Dalton Trans. *1988*, 2555.
34. Fontaine X. L. R., Fowkes H., Greenwood N. N., Kennedy J. D., Thornton-Pett M.: J. Chem. Soc., Dalton Trans. *1987*, 1431.
35. Bown M., Fontaine X. L. R., Kennedy J. D.: J. Chem. Soc., Dalton Trans. *1988*, 1467.
36. Fontaine X. L. R., Greenwood N. N., Kennedy J. D., MacKinnon P., Thornton-Pett M.: J. Chem. Soc., Dalton Trans. *1988*, 2809.
37. Wiliams R. E.: Inorg. Chem. *10*, 210 (1971); Adv. Inorg. Chem. Radiochem. *18*, 67 (1976).
38. Wade K.: J. Chem. Soc., Chem. Commun. *1971*, 792; Adv. Inorg. Chem. Radiochem. *18*, 1 (1976).
39. Nestor K., Štíbr B., Kennedy J. D., Thornton-Pett M., Jelínek T.: Collect. Czech. Chem. Commun. *57*, 1262 (1992).
40. Bould J., Kennedy J. D., Thornton-Pett M.: J. Chem. Soc., Dalton Trans. *1992*, 563.
41. Garret P. M., George T. A., Hawthorne M. F.: Inorg. Chem. *8*, 2008 (1969).
42. Faridoon, Ni Dhubhgaill O., Spalding T. R., Ferguson G., Kaitner B., Fontaine X. L. R., Kennedy J. D.: J. Chem. Soc., Dalton Trans. *1989*, 1657.
43. Bown M., Plešek J., Baše K., Štíbr B., Fontaine X. L. R., Greenwood N. N., Kennedy J. D.: Magn. Reson. Chem. *27*, 947 (1989).
44. McFarlane W.: Proc. R. Soc. London, A *306*, 185 (1968).
45. Clegg W.: Acta Crystallogr., A *37*, 22 (1987).
46. Sheldrick G. M.: *SHELX 76. Program System for X-Ray Structure Determination.* University of Cambridge, Cambridge 1976.
47. Johnson C. K.: *ORTEP II. Report No. ORNL-5138.* Oak Ridge National Laboratory, Tennessee 1976.

Translated by the author (B. Š.).